The development of a novel and powerful biosynthesis platform for expressing huperzine A for the Alzheimer's disease

Han Wen-Xia
Xi'an Medical University
ORCiD: https://orcid.org/0000-0001-7779-2550

Han Zhong-Wen
Fushan hospital of traditional Chinese medicine of tumor

Jia Min
Xi'an Medical University

Zhang Han
Xi'an Medical University

Li Wei-Ze
Xi'an Medical University

weizeli@126.com*Corresponding Author*
ORCiD: https://orcid.org/0000-0002-4688-2112

Yang Li-Bin
Xi'an Medical University

Liang Fei
Xi'an Medical University

Han Lu
Xi'an Medical University

Zhao Ning
Xi'an Medical University

Li Xiao-Feng
Xi'an Medical University

10.21203/rs.3.rs-24161/v1

SUBJECT AREAS

Applied & Industrial Microbiology

KEYWORDS

Huperzine A, Alzheimer's disease, Huperzia serrata, Endophytic fungus, Biosynthesis

Abstract

Background Huperzine A is an important drug for treating Alzheimer's disease and mainly extracted from the Huperzia serrata . Nevertheless, the content of Huperzine A in Huperzia serrata is very low of 0.007% with growing circle of 8 to 10 years, and the chemical synthesis of Huperzine A still has some insurmountable limitations in the industrialized production. So, the available resources of Huperzine A for clinical treatment of Alzheimer's disease are scarce. The purpose of this work was to construct a biosynthesis platform based on the endophytic fungi from Huperzia serrata .

Methods Based on the morphological characteristics and nuclear ribosomal DNA ITS sequences of endophytic fungi to complete the strain identification. Combined alkaloid precipitation with acid dye colorimetry, thin layer chromatography, high-performance liquid chromatography, liquid chromatography-tandem mass spectrometry analysis and inhibition activity of acetylcholinesterase determination model to determine the physicochemical properties of the biosynthetic products. Compare the biosynthetic HupA with the listed APIs of HupA by the test of AChE inhibition ability and cytotoxicity in vitro.

Results In this work, five endophytic fungi Mucor racemosus NSH-D, Mucor fragilis NSY-1, Fusarium verticillioides NSH-5, Fusarium oxysporum NSG-1 and Trichoderma harzianum NSW-V were firstly found and isolated from the Chinese folk medicine Qian Ceng Ta (Huperzia serrata (Thunb.) Trevis. (Lycopodiaceae)), which were identified according to their morphological characteristics and nuclear ribosomal DNA ITS sequences. These fungi could effectively biosynthesize huperzine A in liquid culture of 100-400 mg/L which were 1 000 times higher than that of other reported conventional endophytic fungi. Moreover, these fungi with higher hereditary stability could possess the initial express ability of HupA after 40 generations, and the expressed HupA from these biosynthesis systems has the prior physicochemical properties, better inhibition activity of acetylcholinesterase and lower cytotoxicity compared to the listed APIs of HupA.

Conclusions These results indicate that the endophytic fungi in this work provide a promising alternative platform for producing HupA at industrial scale by biosynthesis for the treatment of Alzheimer's disease.

Introduction

Alzheimer's disease (AD) is a neurodegenerative disease characterized by progressive dementia, which with a death rate about 71% in 7 to 10 years after the onset of the disease and has been recognized as a global public health priority by the WHO (Robert Perneczky 2018). There were about 47 million AD patients worldwide according to the statistical data of WHO in 2017. Due to the ageing population, its prevalence is expected to nearly triple worldwide by 2050 (Robert Perneczky 2018; Gaudreault R and Mousseau N 2019; Maria João Ramalho *et al*., 2020). While, for the AD patient the annual total costs per patient varied from US$2935 to US$64168. So, the AD has already brought tremendous economic burden on the aging society as also as on the family (Robert Perneczky 2018). Although AD has been defined for about 100 years by clinics, however, its molecular mechanism and pathogenesis are still not fully understood. A lot of attempts to find new drug and attack AD based on novel mechanisms such as deposition of β-amyloid (Aβ) and hyperphosphorylated tau have so far failed with numerous phase 3 clinical trials (Justin M. Long *et al*., 2019; Wu X *et al*., 2019), despite many researches and development teams in pharmaceutical companies have devoted great enthusiasm and energy to research. Currently, the most effective treatment for AD is still to enhance cholinergic neurotransmission in the brain and reduce acetylcholine hydrolysis. Fortunately, acetylcholinesterase (AChE) inhibitors are the most effective mechanism for the treatment of AD in clinical (Kunal Roy 2018). Huperzine A (HupA) is one of the AChE inhibitors, which mainly derived from the Chinese folk medicine Qian Ceng Ta (*Huperzia serrata* (Thunb.) Trevis. (Lycopodiaceae). (*HS*)) (Xiaoqiang Ma *et al*., 2008; Ratia M. *et al*., 2013; Xiao-Tian Huang *et al*., 2014). Due to its unique pharmacological activities such as modification of beta-amyloid peptide, reduction of oxidative stress, anti-inflammatory, anti-apoptotic and regulation of nerve growth factor and low toxicity (Orhan I.E. *et al*., 2011; Ying Wang *et al*., 2013), moreover, HupA can increase the α-secretase activity in vitro, decrease the Aβ levels and block the Aβ production (Peng Y *et al*., 2006). These advantages implying the HupA still have a promising future in AD treatment (Yuan HD *et al*., 2016; Andrade S *et al*., 2019). Unfortunately, HupA content in the *HS* is very lower (ca. 0.007%) and the growing circle of the plant is 8 to 10 years (Hongchao Zhang *et al*., 2012), coupled with the chemical synthesis has limitations that

are difficult to overcome such as complexity, high cost, combining with the byproduct, purification difficulties and more potential toxicity in clinical application (Qian L *et al*., 1989; Xia Y *et al*., 1989; Xiaoqiang Ma *et al*., 2008; Shao H *et al*., 2009; Guan-Hua Du 2018). As a result, the available resources of HupA for the increasing AD treatment are scarce and expensive in clinical. Biosynthesis, is a new technology that using microorganisms to synthesize and express the intended drug molecules and with low costs, controllable production process and no pollution production (Stierle A *et al*., 1993; Zhejian Wang *et al*., 2015), and are therefore currently in the research focus. In recent years, a few reports on the isolation of HupA-producing endophytic fungi from different *Huperiaceae* plants have been reported, such as *Acremonium* sp. 2F09P03B, *Blastomyces* sp., *Botrytis* sp., *Blastomyces* sp. HA15, *Shiraia* sp. Slf14, *Cladosporium cladosporioides* LF70, *Aspergillus flavus* LF40, *Paecilonmyces tennis* YS-13, *Xylariales* SY-02, *Colletotrichum gloeosporioides* ES026, *Trichoderma* sp. L44, *Ceriporia lacerata* MY311, *Hypoxylon investiens* MY183, *Alternaria brassicae* AGF041, *Fusarium* sp. Rsp5.2, *Fusarium* sp. C17 (Li W *et al*., 2007; Ju Z *et al*., 2009; Ju Z *et al*., 2009; Ju Z *et al*., 2009; Ya Wang *et al*., 2011; Zhi Bin Zhang *et al*., 2011; Wang Y *et al*., 2011; Su JQ 2011; Su JQ 2011; Shaohua Shu *et al*., 2014; Li-Hui Dong *et al*., 2014; F. F. Zhang *et al*., 2015; F. F. Zhang *et al*., 2015; Amira G. Zaki *et al*., 2019; Thanh Thi Minh Le *et al*., 2020; Olga Lidia Cruz-Miranda *et al*., 2020). However, the output of HupA from these reported fungi is very low and these fungi are very susceptible to mutation and lost the initial express ability of HupA, this are the main obstacles to HupA biosynthesis at an industrial scale. Therefore, active research is the need of the hour toward more efficient strains and synthetic conditions. The aim of our present study was to construct a biosynthesis platform based on mighty endophytic fungi from *HS*, and the characteristics of the constructed biosynthesis platform and the produced HupA were also investigated. This work provides a rather compelling evidence for the HupA biosynthesis having a promising prospect by using these biosynthesis systems developed in this study.

Materials And Methods

2.1 Materials

The whole plant of *HS* was collected from Guangyuan, Sichuan Province. Solvents used for

chromatography were of high-performance liquid chromatography (HPLC) grade. All other reagents were all analytical reagent grade. Standard HupA (SHA, C99% purity) was purchased from Shanghai Siyu Bio-technology CO., LTD., Shanghai, China. AChE, acetylthiocholine iodide (ATCI), and dithiobis nitrobenzoic acid (DTNB) were purchased from Sigma. All other chemicals were from China Medicine Shanghai Chemical Reagent Co. Ltd. PCR primers were synthesised by Shanghai Sangon Biologic Engineering Technology and Service Co. Ltd. Glucose potato nutrient Agar (PDA) was prepared in laboratory.

Male Sprague–Dawley (SD) rats (200–220 g each weight) and rat pheochromocytoma PC-12 cell line were derived from the Animal Center of The Northwest University (Shaanxi, China). All male SD rats were housed in stainless steel cages in a room maintained in a 12 h light/dark cycle at around 22℃ with water and food available ad libitum in the Life Science Research Center at Xi'an Medical University. Rats were allowed to acclimatize for at least 5 d prior to the experiment. Rat pheochromocytoma PC-12 cell line was cultured in RPMI 1640-based medium supplemented with 10% new-born calf serum. All cells were passaged every 5 d, with the cultured condition at 37℃ in an atmosphere of 95% air/5% CO_2 saturated with H_2O. All experiments were carried out 24 h after the cells were seeded.

2.2 Isolation and purification of endophytic fungi from *HS*

Isolation and purification of endophytic fungi from the roots, stems and leaves of *HS* were acquired according to a published method until purified endophytic fungi being obtained (Shen P *et al*., 2000; Changli Min *et al*., 2013; Li-Hui Dong *et al*., 2014; Shaohua Shu *et al*., 2014; Humeera Nisa *et al*., 2015). The purified endophytic fungi were cultured in potato liquid media (28℃, 120 r/min, 5 d) and 3 repeats were set up. Then the culture filtrate was smashed by ultrasonic for 30s and harvested by centrifugation at 12,000×g for 15 min, then the centrifugal supernatant collected for the determination of alkaloids and acid dye colorimetry. The purified strains were cultivated on PDA at 4℃ after that were stored in 15 % glycerine at -80℃.

2.3 The characteritics of HupA

2.3.1Alkaloid precipitation

Select bismuth potassium iodide, potassium iodide mercury and silicotungstic acid as the total alkaloids determination reagent. After the fermentation, take 3.0 mL centrifugal supernatant in a tube and add 3 drops of reagent respectively, observe whether appearing precipitation or not after standing for 30 min. Alkaloids may exist if the precipitation is produced.

2.3.2 Acid dye colorimetry

After the fermentation, pick up 1.0 mL centrifugal supernatant pouring into the separation funnel containing 5.0 ml glacial acetic acid, join 3.0 mL bromocresol green (BCG) solution into it, add water to 10 mL, shake well, then measure chloroform 10 mL accurately access to the above solution, divide the lower chloroform liquid after vibrating 2 min and standing for 1 h. Measured the value of absorbance at 415 nm using the supernatant fluid of PDA medium as control. Alkaloids may exist if the values is plus.

2.3.3 Preparation of extracts

The extracts were prepared by extraction method as previously reported (Shaohua Shu *et al*., 2014). Briefly, the centrifugal supernatant of fermentation solution after ultrasonication was modulated the PH to 3.0 with HCl, and static for 2 h at room temperature, after centrifuging again which was alkalized with $NH_3 \cdot H_2O$ to pH 9.0. Then the solution was extracted three times with chloroform to obtain the combined chloroform extracts which were dried by the rotary evaporator, and after that the obtained residues were dissolved in 5 mL 2.0% HCl and extracted three times with diethyl ether to combine aqueous layer extracts which were dried by the rotary evaporator, then alkalized and extracted as above, the obtained extracts were reconstituted into 5mL methanol and filtered through a syringe filter (0.45 μm) for thin layer chromatography (TLC), high performance liquid chromatography (HPLC) and liquid chromatography-tandem mass spectrometry (LC-MS/MS) analysis. Each sample was analyzed in duplicate.

2.3.4 TLC

TLC was detected according to a published method with some modifications (Zhi Bin Zhang *et al*., 2011; Li-Hui Dong *et al*., 2014). Conditions were: chloroform/acetone/isopropanol (4:4:2) as developer; 0.3 % potassium hypermanganate solution as color reagent. Sample and SHA with 0.4 μl

were dripped by using a capillary at 1 cm away from one end of the plate. After drying, the plate was placed in a developing solution at room temperature. Then the TLC plates were naturally dried and the color reagent was sprayed, and the number of spots and Rf values were recorded.

2.3.5 Qualitative and quantitative by HPLC and LC-MS/MS

HupA content was measured by HPLC using an Agilent HPLC 1100 series (Agilent, Santa Clara, CA, USA) consisting of a C18 column (4.60 mm×250 mm, 5 μm; Shimadzu, Tokyo, Japan). The temperature of the column compartment was maintained at 25℃. The flow rate was 1.0 mL/min using methanol-0.1% formic acid (75:25, v/v) as the mobile phase. Samples of 20 μL were loaded for detection at 310 nm (Zhi Bin Zhang *et al*., 2011; Shaohua Shu *et al*., 2014). Quantification was achieved by using the standard curve generated from SHA, which linear in the range of 0.003-0.05 mg/mL and with r^2=0.9996, after that HupA from endophytic fungi (FHA) was further identified by mass spectroscopy analysis using the electrospray technique with an Agilent 1260-6460A LC-MS/MS. The sample purified by TLC was dissolved in 100% HPLC grade methanol and was injected with a spray flow 400 μL/min.

2.3.6 Inhibition activity of AChE by determination model

Inhibition activity of AChE about HupA was detected according to a published method with some modifications (Andrew Marston *et al*., 2007; Cheng X *et al*., 2008; Zelik P *et al*., 2009): 125 μL of 0.1 mol/L PBS, 50 μL of 0.4 U/mL AChE, 25 μL of 7.6 mmol/L DTNB, 20 μL of FHA (0.05mg/mL), 20 μL of phytoextraction HupA (PHA) (0.05 mg/mL), 20 μL of SHA (0.05 mg/mL) were placed on a 96-well plate, at the same time set up blank control. The plate was shaken fully and kept at 30℃ for 30 min. Then 30 μL of 6.2 mmol/l ATCI were added to the tube for the development of colour reaction. After that, the metabolites in the mixture were detected on the enzyme labeling meter at 412 nm (Bruhlmann C *et al*., 2007). The above test are repeated three times and the PHA and SHA used as controls.

2.4 Biological identification

2.4.1 Morphological identification of strains

The strains of the endophytic fungi were inoculated onto PDA media at 26-28℃ for 5 d and the morphologies were preliminary characterized with the size, shape and color of the colonies, and more

with the mycelia, conidia, pycnidia, etc. observed by light microscope (eclipse 55i, Nikon, Japan) and scanning electron microscope (SEM, QUANTA-200F, FEI, Netherlands) according to the Fungal Identification Manual (Wei JC 1979; Ainsworth GC 2008).

2.4.2 Molecular identification of strains

The genomic DNA of fungi were extracted according to a reagent kit. Specific primers ITS1 (5´-TCCGTAGGTGAACCTGCGG-3´) and ITS4 (5´- TCCTCCGCTTATTGATATGC -3´) were designed according to the conserved sequences of some known fungi (Li-Hui Dong *et al*., 2014); ITS segments were amplified with the genome DNA as template. Construct PCR system (25 μL): template (genome) 0.5 μL, 10×Buffer（with Mg^{2+}）2.5 μL, dNTP 1.0 μL, Taq enzyme 0.2 μL, primers (10 μmol/L) each 0.5 μL, addition of water to 25 μL. Reaction conditions: initial denaturation at 94℃ for 4 min; cycling at 94℃ for 45 Sec, 55℃ for 45 Sec, 72 ℃ for 1 min, 30 cycles; extension for 10 min. PCR products were detected by using 1% gel electrophoresis, and sequenced by Sangon biological engineering co., LTD. Shanghai. The sequences were submitted to GenBank and were assigned with accession numbers.

2.4.3 Phylogenetic analysis of ITS

The similarities of the measured ITS sequences of endophytic fungi was compared by the blast. Evolutionary analyses were conducted in MEGA 7. The evolutionary history was inferred using the Neighbor-Joining method, with 1,000 bootstrap replications, and the evolutionary distances were computed using the Maximum Composite Likelihood method and are in the units of the number of base substitutions per site.

2.4.4 Hereditary stability and yielding of HupA

The heritage stability of strains was studied by continuous passages. The wild strains producing HupA were cultured in potato glucose liquid medium with consistent fermentation conditions after tube passage. The ability of wild strains producing HupA was investigated after the 5th, 10th, 15th, 20th, 25th, 30th, 35th and 40th passage, with the interval 1 month between generations. The yield of HupA from the strains was determined by HPLC as above mentioned.

2.5 Determinate the AChE activity and the cytotoxicity of HupA in vitro

2.5.1 Determinate the AChE activity in vitro

AChE activity assay was investigated by using a reagent kit. The SD rats were divided into 4 groups after acclimatized to the facilities for 5 days. Group-A: animals without any treatment, food and water were available ad libitum, for 10 d. Group-B: animals were orally administrated SHA, the dosage of HupA was 0.2 mg/kg, for 10 d. Group-C: administrated PHA, the dosage regimen as above. Group-D: administrated FHA and the dosage regimen as above. During the whole experiment, the rats were housed in stainless steel cages in an air-conditioned room maintained in a 12h light/dark cycle at around 22h with food and water available ad libitum. At the last, the rat's brain samples were obtained, washed by physiological saline and blotted by filter paper then frozen at −20℃ until analysis. The brain tissue was homogenized by a hand-held laboratory homogenizer with 9ml physiological saline after that which was centrifuged at 5000 rpm for 5 min. The AChE inhibition assay was taken out according to the manufacturer's protocol with using the 10% brain homogenate as enzyme source. The optical density at 412 nm (OD 412 nm) was determined by a microplate reader. The activity of AChE (U/mgprot) in this work means hydrolyzed 1.0 mol groundsubstance of reaction system by 1.0 mg brain tissues at 37℃ for 6 min as one unit of activity. This study was approved by the animal ethics committee of Xi'an Medical University.

2.5.2 Evaluation the cytotoxicity

Rat pheochromocytoma PC-12 cell line was used to investigate the cytotoxicity of FHA. The PC-12 cells were seeded into 96-well microplates at a density 10^5 cells/mL. The cytotoxicity was evaluated by the lactate dehydrogenase (LDH). After seeding in 96-well microplates for 24 h, cells were incubated for 12 h with SHA, PHA and FHA, respectively. Then cell-free culture supernatants were carefully aspirated and collected for LDH determination according to the reagent kit. The optical density was measured at 450 nm (OD450 nm) by a microplate reader. All data were presented as means ± S.D. of numbers obtained from six wells and three separate experiments. Normal untreated PC-12 served as controls. This study was approved by the animal ethics committee of Xi'an Medical University.

2.6 Statistical analyses

All results were expressed as the mean ±S.D. which were analyzed by one-way analysis of variance

and two-tailed Student's t-test using SPSS13.0; the p-value of less than 0.05 was considered significant.

Results

3.1 The isolated endophytic fungi from *HS*

The resources of endophytic fungus are abundant in the wild *HS.* As shown in Fig.1, a total of 26 endophytic fungi were carefully isolated from the leaves, stems and roots of wild *HS*. And different endophytic fungi presented different morphology characterization, indicating each endophytic fungus has a unique genetic characteristic which would cause different expressions. While, no fungal growth was observed on the control media.

3.2 HupA-producing endophytic fungi from *HS*

During the process of alkaloid screening, we had found that the combination of alkaloid precipitation and acid dye colorimetry was more efficient than using a single method. As shown in Fig.2, nineteen of the 26 strains could produce precipitation by potassium mercuric iodide (Fig.2A), seven strains could produce precipitation by bismuth potassium iodide (Fig.2B). And five strains of 3, 8, 15, 16 and 17 could produce obvious precipitation by silicotungstic acid (Fig.2C). What is more, these five strains could generate absorbance at 415 nm compared with the complex compound of BCG and HupA (HupA-BCG) (Tab.1), and the higher the absorbance content of strain fermentation broth, the more possible it could product HupA. As a result, the TLC showed the fungal compounds which produced by the five strains of 3, 8, 15, 16 and 17 exhibited the same color spots and R_f values as SHA (Fig. 3A and B). And more the metabolites of the five strains above mentioned had the pretty much same retention time as SHA by HPLC (Fig. 4). Strain 3 showed a peak with retention time 8.803 min (Fig. 4B), strain 8 with 8.825 min (Fig. 4C), strain 15 with 8.806 min (Fig. 4D), strain 16 with 8.629 min (Fig. 4E) and strain 17 with 8.419 min (Fig. 4F), which were all be identical to the 8.506 min of SHA at the same chromatographic conditions (Fig. 4A). The peak times all overlaped when the SHA was added. All of these results demonstrated that the five strains of 3, 8, 15, 16 and 17 have the powerful express ability of HupA. Meanwhile, the FHA yielded a peak $[M-H]^-$ at *m/z* 240.11, $[M-NH_2]^-$ at *m/z* 223.81(Fig. 5b) by LC-MS/MS assays, which were same as the characteristic peaks $[M-H]^-$ at *m/z*

240.11 and $[M\text{-}NH_2]^-$ at *m/z* 223.71 of SHA (Fig. 5a), this verified again that the five strains above mentioned had did produce HupA as expected.

Tab.1 Optical absorbency of alkaloid-BCG at 415 nm

Strain number	value of A_{415}
3	0.281±0.041
8	0.482±0.052
15	0.392±0.008
16	0.053±0.070
17	0.402±0.030
HupA-BCG	0.501±0.021

Notes: The absorbance of different strains at 415nm for 3, 8, 15, 16, 17 and HupA-BCG.

3.3 Detection of inhibition activity of AChE

It is clearly demonstrated in Fig.6 that the biosynthetic FHA by the strains of 3 (A), 8 (B), 15(C), 16 (D) and 17(E) were all caused obvious AChE inhibition activity, and the inhibition increased with the response time. In addition, the AChE inhibition effect of the biosynthetic FHA was better than that of PHA and SHA (*t*-test, $P < 0.05$) (F). The reason may be that the biosynthetic FHA has higher purity and better conformation, followed by a desired efficacy and lower unintended side effects. As a general guide, a desired efficacy and lower unintended side effects are beneficial to patients who need long-term HupA therapy. Taken together, these results suggested that the five endophytic fungi have the good performance characteristics as expected for constructing biosynthesis platform for HupA for the AD applications.

3.4 Identification of HupA-producing strains

3.4.1 Morphological characteristics

The five HupA-producing strains as above mentioned were cultivated in PDA medium. As shown in Fig.7, the strain 3 grew rapidly and covered up to 7 cm after 3 d until spreading out the whole PDA medium after 5 days at 26℃. The hyphae were loose and brown with exudate on the surface, which spread forming an irregular colony edges on the upside of the medium while the backside was brown (Fig.7A-D). It can be clearly seen sporangiophore diameter of 5-35 μm was uniaxial branching through light microscope and SEM (Fig. 7E-1, F-4). Septate hypha was shown in Fig. 7F-2. Spore sac in the

sporangium phase with a diameter of 25-65 μm (Fig. 7F-1, G-1) was small volume as a young (Fig. 7I-1), and the older it was the more easily the wall to be fully broken (Fig. 7H). Intensive aerial hyphae diameter of 10-20 μm (Fig. 7G-2), spore diameter of 40-50 μm was almost spherical or short oval (Fig. 7J). Spherical zygosperm diameter of 70-80 μm had small warts on the surface (Fig. 7K). Chlamydospore diameter of 10-20 μm formed from hypha and sporophore (Fig. 7E-2, F-3, I-2). Thallospore on the sporophore formed as a short oval (Fig. 7L). Based on the morphological characteristics it was initially classified into *Mucor racemosus* according to Ainsworth's classification of fungi (Wei JC 1979; Ainsworth GC 2008), which was named as *Mucor racemosus* NSH-D according to the collection place of the *HS*.

As shown in Fig.8, the strain 8 produced air-generated hypha with a diameter of 2-3 μm cultivated in PDA medium at 26℃, which was loose and hair-like with a fast growth rate for spreading across the whole medium after 4 d. The center of the colony on the upside was white fuzz at first and then to be brown after 4 d with the height of 5-20 mm (Fig.8A, C), while the backside was milky white (Fig.8B, D). Light microscope and SEM images revealed that the hypha was aseptate (Fig.8E, F-3); single sporophore diameter of 30-50 μm was standing upright look like long cylinders with acrogenous sporangium (Fig.8F-2) and no sterigmata branch (Fig.8F-1,G), from the base of which short branch of sporangiole appear occasionally (Fig.8F-4,5H); conidia forming in the thin-walled sporangium which attached to the sporophore (Fig.8I-1, J-1) with the cylindrical shape initially then formed to be a series of sporangiospore (Fig.8J-2, J-3) were released from the broken sporangium (Fig.8K-1); sporangiospore was spherical with diameter of 1-1.5 μm or ovoid with the aspect ratio of 2:1 or 3:1 (size of 6-8×3-4 μm) (Fig.8I-2, I-3, K-2, K-3, K-4); zygospore born in the hyphae and zygamgium had been completed the process of zygo as shown in Fig.8L, while zygamgium was going to zygo as shown in Fig.8M; chlamydospore was acrogenous usually, smooth, spherical and colorless (Fig.8N). Based on the morphological characteristics it was initially classified into *Mucor fragilis* according to Ainsworth's classification of fungi (Wei JC 1979; Ainsworth GC 2008) which was named as *Mucor fragilis* NSY-1 according to the collection place of the *HS*.

As shown in Fig.9, the strain 15 produced air-generated hyphae with a diameter of about 3.5 μm

at 27℃ on the PDA medium, which were dense, developed and cotton-like with a growth rate for spreading across the medium up to 6.0 cm after 5 d. The surface of the colony with the height of 5-10 mm was pale and flocculent on the upside while for the backside it was dark brown on the center and light brown at the edge (Fig.9A, B, C, D). It was clearly visible under light microscope and SEM that the conidiophore with the size of 55-125 μm long and 3.2-4.8 μm wide was born from the aerial hyphae (Fig.9E-1, I-2) which was unbranched or rotate-branched (Fig.9E-2), bearing apical conidia arranged in chains (Fig.9E-3, F) or formed false heads (Fig.9I-1, J) from the single conidiophore. Septate hypha was shown in Fig.9G. Different size of conidia shown in Fig.9H, a few great conidia were sickle-shaped which were slender in the middle and slightly curved at both ends with the size of (20.1-35.9) × (2.8-4.2) μm and containing 3-6 septate parenchyma cells (Fig.9H-1), while microconidia were numerous and variously shaped such as ovoid or clavate with the size of (4.3-10.5) ×(2.0-3.1) μm and containing 1-2 septate parenchyma cells (Fig.9H-2, K, L). Based on the morphological characteristics, it was initially classified into *fusarium verticillioides* according to Ainsworth's classification of fungi (Wei JC 1979; Ainsworth GC 2008) which was named as *fusarium verticillioides* NSH-5 according to the collection place of the *HS*.

As shown in Fig.10, the strain 16 produced air-generated hyphae with a diameter of about 3.5 μm at 26℃ on the PDA medium, which were dense, developed and cotton-like with a growth rate for spreading across the medium up to 6.6 cm after 5 d. The surface of the colony with the height of 5-10 mm was pale and flocculent on the upside while for the backside it was dark brown on the center and light brown at the edge (Fig.10A, B, C, D). It was clearly visible under light microscope and SEM that the conidiophore with the size of 25-120 μm long and 2.6-3.2 μm wide was born from the aerial hyphae (Fig.10J, M-1) which was unbranched (Fig.10E-2, I) or rotate-branched (Fig.10E-1, M-1). Septate hypha was shown in Fig.10F-1. Different size of conidia shown in Fig.10, a few scattered great conidia were sickle-shaped which were slender in the middle and slightly curved at both ends with the size of (12.2-22.9)×(2.6-3.9) μm with single spore (Fig.10F-3, G, L-1), while numerous scattered microconidia were variously shaped such as slightly curved ovoid or clavate with the size of (2.1-6.5)×(1.8-2.7) μm and with single spore (Fig.10F-2, H, L-2), meanwhile some of these were

inserted on the apex of a single conidiophore (Fig.10K). Acrogenous chlamydospore was spherical and smooth as shown in Fig.10M-2, N. Based on the morphological characteristics; it was initially classified into *fusarium oxysporum* according to Ainsworth's classification of fungi (Wei JC 1979; Ainsworth GC 2008) which was named as *fusarium oxysporum* NSG-1 according to the collection place of the *HS*.

As shown in Fig11, the strain 17 produced air-generated hyphae with a diameter of 1-10 μm cultivated in PDA medium at 28℃, which were intensive and felt-like with a fast growth rate for spreading across the whole medium after 4 d. The center of the colony on the upside was ashen at first and then to be dark green (Fig.11A, C), while the backside was ashen (Fig.11B, D). It can be clearly seen the septate hyphae (Fig.11F-1) were slender colorless at first then to be grayish with diameter of 1-1.5 μm and with many branches through light microscope and SEM (Fig.11F-2). Conidiophore diameter of 2-4 μm was born from the lateral branches of aerial hyphae (Fig.11E-1) that presented as bifurcate (Fig.11H-1) or trifurcate branchlets, of which often opposite (Fig.11E-3, G-3) or alternate (Fig.11E-2G-1, H-2) and its apex was not enlarged clustering the upper conidia head (Fig.11G-2, H-3). The minor conidiophore was bottle-shaped (Fig.11 I-1, K-2) or cone-shaped from which conidia were inserted (Fig.11 I-2, K-1). Conidia were mostly spherical and blue-green (2-4 μm in diameter) (Fig.11J-1, J-2, K-3, L-1), with small warts on the spore walls (Fig.11L-2). Based on the morphological characteristics it was initially classified into *Trichoderma harzianum* according to Ainsworth's classification of fungi (Wei JC 1979; Ainsworth GC 2008), which was named as *Trichoderma harzianum* NSW-V according to the collection place of the *HS*.

3.4.2 Molecular identification of the isolated strain

With ITS1 and ITS4 as primers, the genome DNA of strain NSH-D, NSY-1, NSH-5, NSG-1, NSW-V were amplified successfully and detected by agarose gel electrophoresis carefully. The results showed that the amplification band sizes were about 500-750 bp, 500 bp, 500 bp, 1200-1500 bp, 500-600 bp for the NSH-D, NSY-1, NSH-5, NSG-1 and NSW-V respectively, and there were no heterozygosis (Fig.12A, B). What is moreno changes were observed in the sequence analysis of fungal rDNA ITS after the 40 passages of the stains indicating the genome DNA for these strains has a relatively

higher stability, this is beneficial for HupA biosynthesis at an industrial scale.

3.4.3 Phylogenetic analysis of ITS

Using ITS1 and ITS4 as primers, the DNA recovered by agarose gel electrophoresis were analyzed for ITS-rDNA sequence, and fragments of 638 bp, 546 bp, 532 bp, 1301 bp, 551 bp were obtained respectively for the strains of NSH-D, NSY-1, NSH-5, NSG-1, NSW-V, which were submitted to GenBank (accession numbers: KX060585, KX060586, KX853851, KX853850, KX034080). These sequences were further compared by Blast on NCBI. The evolutionary tree were constructed by using MEGA 7.0 software with ClustalW method and Neighbour-joining method, and the Bootstrap value of self-expansion test were labeled on the branches for 1,000 times, and the results of evolutionary tree construction were shown in Fig. 13. As a result, the NSH-D ITS-rDNA sequence was found to be 99% similar with *Mucor racemosus* F13J-1 (accession number KJ911288.1) and *Mucor racemosus* xsd08071 (accession number FJ582639.1), indicating the strain NSH-D and *Mucor racemosus* had close evolutionary distance in the phylogenetic tree (Fig.13A). So, in this study the strain NSH-D was identified as *Mucor racemosus* NSH-D by combining morphological analysis and ITS sequence analysis. The ITS-rDNA sequences of strain NSY-1 was 100% similarity with *Mucor* sp. CFEF005 (accession number KF158220.1) and *Mucor* sp. KACC 46076 (accession number JN315018.1), 99% with *Mucor fragili*s strain CBS 236.35 (accession number FN650655.1) and *Mucor fragilis* LS266 (accession number JQ972063.1), indicating the strain NSY-1 and *Mucor fragili*s had close evolutionary distance in the phylogenetic tree (Fig.13B). Therefore, the strain NSY-1 was identified as *Mucor fragilis* NSY-1 by combining morphological analysis and ITS sequence analysis in this study. The NSH-5 ITS-rDNA sequence was found to be 100% similar with *Fusarium verticillioides* BPFus 01 (accession number KM434131.1) and *Fusarium* sp. BPEF75 (accession number KF151850.1), indicating the strain NSH-5 and *Fusarium verticillioides* had close evolutionary distance in the phylogenetic tree (Fig.13C). The strain NSH-5 was identified as *Fusarium verticillioides* NSH-5 by combining morphological analysis and ITS sequence analysis accordingly. The ITS-rDNA sequences of strain NSG-1 was 100% similarity with *Fusarium* sp. MF511 (accession number KM096318.1) and *Fusarium* sp. MBS1 (accession number FJ613599.1), 99% with *Fusarium oxysoporum* K14 (accession number JF807402.1), indicating the

strain NSG-1 and *Fusarium oxysoporum* had close evolutionary distance in the phylogenetic tree (Fig.13D). So, the strain NSG-1 was identified as *Fusarium oxysoporum* NSG-1 by combining morphological analysis and ITS sequence analysis. The NSW-V ITS-rDNA sequence was found to be 100% similar with *Trichoderma harzianum* BHR2P1F3M (accession number KF986661.1) and *Trichoderma harzianum* JSB22 (accession number KC569353.1), indicating the strain NSW-V and *Trichoderma harzianum* had close evolutionary distance in the phylogenetic tree (Fig.13E). And the strain NSW-V was identified as *Trichoderma harzianum* NSW-V by combining morphological analysis and ITS sequence analysis.

3.4.4 Results of hereditary stability and yielding of HupA

The ability of the wild strain NSH-D, NSY-1, NSH-5, NSG-1, NSW-V producing hupA were determined after 5th, 10th, 15th, 20th, 25th, 30th, 35th and 40th passage. After 40 passages, there were no significant difference between the strain and the wild strain of the ability producing hupA (*t*-test, $P>0.05$) as shown in Tab.2. These results also indicated again that these strains have a relatively higher stability for continuously expressing HupA.

Tab.2 The batches stability results of the five strains

Passage number	FHA for NSH-D (mg/L)	FHA for NSY-1 (mg/L)	FHA for NSH-5 (mg/L)	FHA for NSG-1 (mg/L)	FHA for NSW-V (mg/L)
0	106.0	181.5	117.6	111.0	320.0
5	108.0	183.2	116.9	110.6	320.5
15	105.2	181.9	117.0	112.0	319.5
20	109.0	182.2	116.5	111.4	319.0
25	107.2	180.3	117.0	111.5	320.5
30	106.3	181.0	117.2	110.8	320.0
35	107.4	181.9	117.6	110.5	319.3
40	107.2	182.1	117.0	111.0	319.6

3.5 Animal and cell toxicity test

3.5.1 The AChE inhibition of Hup A produced by fungi in vitro

It is clearly demonstrated in Tab.3 that all of the HupA from different sources could significantly inhibit AChE activity compared to the control, namely group-1 in vitro. Meanwhile, Group-4 indicated higher AChE inhibition compared with group-2 and group-3, with no significant difference (*t*-test, $P>0.05$). The reason may be that biosynthetic pathway has the superiority of efficient and selective mild catalytic system by three possible pathways (chemical selectivity, regional selectivity and stereo

selectivity), and therefore caused better AChE inhibition compared with SHA and PHA.

Tab.3 The AChE activity in rats brain after administrated HupA from different sources. Data were expressed as means ± S.D (n = 3).

Experimental group	Group1	Group2	Group3	Group4				
Group name	Normal	SHA	PHA	FHA (NSH-D)	FHA (NSY-1)	FHA (NSW-V)	FHA (NSH-5)	FHA (NSG-1)
AChE(U/mgprot)	11.5	7.8	7.3	6.8	6.4	6.3	6.6	6.5

Notes: **Group1**: animals without any treatment (Normal); **Group2**: animals were orally administrated standard HupA (SHA); **Group3**: animals were orally administrated phytoextraction HupA (PHA); **Group4**: animals were orally administrated HupA obtained from endophytic fungi (FHA) (FHA-NSH-D, FHA-NSY-1, FHA-NSH-5, FHA-NSG-1, FHA-NSW-V).

3.5.2 Evaluation the cytotoxicity

In this study, it was very important to determine whether the FHA was indeed improving the activity of AChE inhibition rather than loss of cellular viability. PC-12 cell injury was quantitatively evaluated by the determination of LDH which was an indicator of cell injury released from damaged cells. Cultured rat pheochromocytoma PC-12 cells were tested basis on viability after incubation with Hup A from different sources. As shown in Tab. 4, it clearly demonstrated that the released LDH for group4 (FHA) was lower than the group2 (SHA) and group3 (PHA) and with no significant statistical difference among them (*t*-test, $P>0.05$). These results suggest that the PC-12 cells damage caused by FHA was much lower compared to the SHA and PHA. Hence, FHA may be an effective and safe source of crude drug for the AD treatment.

Tab. 4 – The cytotoxicity was determined with the LDH assay, after incubation with HupA from different sources. Data were expressed as means ± S.D (n = 6).

Experimental group	Group1	Group2	Group3	Group4				
Group name	Normal	SHA	PHA	FHA (NSH-D)	FHA (NSY-1)	FHA (NSW-V)	FHA (NSH-5)	FHA (NSG-1)
OD(LDH releaset)	0.035	0.085	0.080	0.073	0.0728	0.0731	0.0725	0.0727

Note: **Group1**: without any treatment (Normal); **Group2**: administrated standard HupA (SHA);

Group3: administrated phytoextraction HupA (PHA); **Group4**: administrated HupA obtained from endophytic fungi (FHA) (FHA-NSH-D, FHA-NSY-1, FHA-NSH-5, FHA-NSG-1, FHA-NSW-V).

Discussion

Microbial secondary metabolites have always been one of the important sources of discovery and development of lots of new drugs due to their remarkable biological activities. In this study, many valuable endophytic fungi were first isolated from *HS,* and the AChE inhibition activity determination model and the cytotoxicity test in vitro were used to evaluate the activities of the metabolites from these endophytic fungi. As evident from these, FHA had better inhibition activity of AChE , and also effectively avoided cell injury. In addition, the endophytic fungi *Mucor racemosus* NSH-D, *Mucor fragilis* NSY-1, *Fusarium verticillioides* NSH-5, *Fusarium oxysporum* NSG-1, *Trichoderma harzianum* NSW-V have never been reported capable of producing HupA. This present study is the first to isolate, characterise, and identify them from *HS* in China which also demonstrates the diversity of endophytic fungi in *HS.* Meanwhile, all of these fungi have great advantages of high product of HupA which were 1000 times higher than others (Tab. 5) and more with hereditary stability after 40 generations. As a result all of these fungi were high yield of HupA, high anti-AChE activity, high hereditary stability that may provide a more safty, more efficient, lower cost and no pollution platform for HupA by biosynthesis, which could be used in treating Alzheimer’s disease and preventing further memory degeneration. The discovery of HupA-producing endophytic fungi is also valuable for both basic research and industrial promising candidate applications for large-scale HupA production. The limitation of the study is that we have not yet understood fully about the mechanism of high production why endophytic fungi could maintain high yields and stable activity when symbiotic with a particular bacterium that was the direction for our further research.

Tab. 5 Yield of HupA reported from different endophtic fungi

Strains	Yield of HupA	Reference	plants
Acremonium sp. 2F09P03B	8.32 μg/L	Li W *et al*., 2007	*HS*
Blastomyces sp.	20-30 μg/g DCW	Ju Z *et al*., 2009	*Phlegmariurus cryptomerianu*
Botrytis sp.	20-30 μg/g DCW	Ju Z *et al*., 2009	*Phlegmariurus cryptomerianu*
Blastomyces sp. HA15	20-30 μg/g DCW	Ju Z *et al*., 2009	*Huperziaceae*
Shiraia sp. Slf14	327.8 μg/L	Ya Wang *et al*., 2011	*HS*
Cladosporium cladosporioides LF70	56.84 μg/g DCW	Zhi Bin Zhang *et al*., 2011	*HS*
Aspergillus flavus LF40	80.1 μg/g DCW	Wang Y *et al*., 2011	*HS*
Paecilonmyces tennis YS-13	21.0 μg/L	Su JQ 2011	*Huperziaceae*
Xylariales SY-02	26.4 μg/L	Su JQ 2011	*Huperziaceae*
Colletotrichum gloeosporioides ES026	1 μg/g DCW	Shaohua Shu *et al*., 2014	*HS*
Trichoderma sp. L44	37.63 μg/g DCW	Li-Hui Dong *et al*., 2014	*HS*
Ceriporia lacerata MY311		F. F. Zhang *et al*., 2015	*Phlegmariurus phlegmaria*
Hypoxylon investiens MY183	40.53 μg/L	F. F. Zhang *et al*., 2015	*Phlegmariurus phlegmaria*
Alternaria brassicae AGF041	42.89 μg/g DCW	Amira G. Zaki *et al*., 2019	*HS*
Fusarium sp. Rsp5.2	2849±2.6 μg/L	Thanh Thi Minh Le *et al*., 2020	*HS*
Fusarium sp. C17	3.2 μg/g DCW	Olga Lidia Cruz-Miranda *et al*., 2020	*HS*

Note: μg/g DCW: HupA per dry weight of mycelium; μg/L: HupA per liquid volume of fermentation liquid.

Conclusions

In this work, the endophytic fungi *Mucor racemosus* NSH-D, *Mucor fragilis* NSY-1, *Fusarium verticillioides* NSH-5, *Fusarium oxysporum* NSG-1 and *Trichoderma harzianum* NSW-V were first isolated from *HS.* These endophytic fungi have great advantages of high product of HupA which were 1 000 times higher than others and more with hereditary stability after 40 generations. In addition, the biosynthesized HupA had better inhibition activity of AChE and also effectively avoided cell injury. All of these results demonstrated that these developed endophytic fungi have been providing a novel powerful biosynthesis platform for expressing HupA for the AD and having a broad application prospect.

List Of Abbreviations

Tab. 6 List of abbreviations

Abbreviations	Full name
HupA	Huperzine A
HS	*Huperzia serrata*
AD	Alzheimer's disease
AChE	Acetylcholinesterase
SHA	Standard HupA
ATCI	Acetylthiocholine iodide
DTNB	Dithiobis nitrobenzoic acid
PDA	Glucose potato nutrient Agar
SD	Sprague–Dawley
BCG	Bromocresol green
TLC	Thin layer chromatography
HPLC	High-performance liquid chromatography
LC-MS/MS	Liquid chromatography-tandem mass spectrometry
FHA	HupA from endophytic fungi
PHA	phytoextraction HupA
SEM	Scanning electron microscope
LDH	Lactate dehydrogenase
HupA-BCG	BCG and HupA

Declarations

Ethics approval and consent to participate

The study protocol was approved by the ethics review board of Xi'an Medical University. All of the procedures were performed in accordance with the Declaration of Helsinki and relevant policies in China. The collection of the *Huperzia serrata* complied with the IUCN Policy Statement on Research Involving Species at Risk of Extinction and the Convention on the Trade in Endangered Species of Wild Fauna and Flora and relevant policies in China. All the experiments in the study were carried out in compliance with relevant institutional biosafety and biosecurity protocols and any national or international recommendations relevant to the research field.

Consent for publication

All authors have seen the manuscript and approved to submit to your journal.

Availability of data and material

The datasets generated and/or analysed during the current study are available in the [NCBI] repository, and data generated or analysed during this study are included in this published article.

Competing interests

The work described has not been submitted elsewhere for publication, in whole or in part, and all the authors listed have approved the manuscript that is enclosed. The manuscript does not infringe any personal or other copyright or property rights.

Funding

This researh work was sponsored by the Youth Innovation Team of Shaanxi Universities (Shaanxi

Education No. 90 [2019]), the general programs of Shaanxi Education Department (Grant No.17JS120), the project association for Science and Technology Youth Talent Lift in Colleges and Universities of Shaanxi Province (Grant No.20170411), the scientific research topics of Shaanxi Administration of Traditional Chinese Medicine (Grant no. 2019-ZZ-ZY010), the general programs of shaanxi Science and Technology department (Grant No. 2020JM-610), field project from Xi'an Medical University (Grant no. 2018PT71, 2018PT72, 2018PT73).

Authors' contributions

HWX was responsible for the design of the whole experiment and carried out the morphological and molecular biology studies and drafted the manuscript. HZW participated in the collection of the *Huperzia serrata.* JM and ZH carried out the preparation of extracts and the test of TLC and HPLC. LWZ was responsible for guiding the research and checking the article. YLB and LF carried out the AChE inhibition ability and cytotoxicity test. HL carried out the test of LC-MS/MS and the study of hereditary stability. ZN participated in the coordination and helped to draft the manuscript. LXF carried out the alkaloid precipitation and acid dye colorimetry and the study of hereditary stability. All authors read and approved the final manuscript.

Acknowledgements

Not applicable.

References

Ainsworth GC (2008) Ainsworth & Bisby's dictionary of the fungi. Cabi, Wallingford.

Amira G. Zaki, Einas H. El-Shatoury, Ashraf S. Ahmed, Ola E. A. Al-Hagar (2019) Production and enhancement of the acetylcholinesterase inhibitor, huperzine A, from an endophytic *Alternaria brassicae* AGF041. *Applied Microbiology and Biotechnology* **103**, 5867–5878.

Ana Ferreira, Márcio Rodrigues, Ana Fortuna, Amílcar Falcão, Gilberto Alves (2016) Huperzine A from *Huperzia serrata*: a review of its sources, chemistry, pharmacology and toxicology. *Phytochemistry Reviews* **15**: 51–85.

Andrade S, Ramalho MJ, Loureiro JA, Pereira MDC (2019) Natural compounds for Alzheimer's disease therapy: a systematic review of preclinical and clinical studies. *Int J Mol Sci* **20** (9):In press.

Andrew Marston, Kurt Hostettmann, Pierre-Alain Carrupt, Bernard Testa, Corinne Bruhlmann (2004) Screening of Non-Alkaloidal Natural Compounds as Acetylcholinesterase Inhibitors. *Chemistry & biodiversity* **1**(6): 819-829.

Changli Min, Xuejun Wang (2013) Isolation and Identification of a Huperzine A-producing Endophytic Fungi from *Huperzia serrata*. *Natural Product Research and Development* **25**: 590-593 (in Chinese).

Cheng X, Chen J, Zhu DY (2008) Initially research in acetylcholinesterase inhibitory activity of endophytic fungi g5 isolated from *Huperzia serrata*. *Microbiol Chin* **35**:1764–1768.

David B, Wolfender JL, Dias DA (2015) The pharmaceutical industry and natural products: historical status and new trends. *Phytochem Rev* **14**(2):299–315.

F. F. Zhang, M. Z. Wang, Y. X. Zheng, H. Y. Liu, X. Q. Zhang, S. S. Wu (2015) Isolation and characterzation of endophytic Huperzine A-producing fungi from *Phlegmariurus phlegmaria.* *Microbiology***84**: 701–709.

Gaudreault R, Mousseau N (2019) Mitigating Alzheimer's disease with natural polyphenols: a review. *Curr Alzheimer Res* **16**(6): 529–43.

Ghulam Md, AshrafAthanasios Alexiou (2019) Biological, Diagnostic and Therapeutic Advances in Alzheimer's Disease. People's Medical Publishing House, Singapore.

Guan-Hua Du (2018) Natural Small Molecule Drugs from Plants. People's Medical Publishing House, Singapore.

Humeera Nisa, Azra N. Kamili, Irshad A. Nawchoo, Sana Shafi, Nowsheen Shameem, Suhaib A. Bandh (2015) Fungal endophytes as prolific source of phytochemicals and other bioactive natural products: A review. *Microbial Pathogenesis* **82**: 50-59.

Ju Z, Wang J, Pan SL(2009a) Isolation and preliminary identification of the endophytic fungi which produce Hupzine A from four species in *Hupziaceae* and determination of Huperzine A by HPLC. *Fudan Univ J Med Sci* **36**(4): 445-449 (in Chinese).

Justin M. Long, David M. Holtzman (2019) Alzheimer Disease: An Update on Pathobiology and Treatment Strategies. *Cell*: In press.

Kunal Roy□2018□Computational Modeling of Drugs Against Alzheimer’s Disease. Humana Press, New

York.

Li-Hui Dong, San-Wei Fan, Qing-Zhi Ling, Bei-Bei Huang, Zhao-Jun Wei (2014) Indentification of huperzine A-producing endophytic fungi isolated from *Huperzia serrata*. *World J Microbiol Biotechnol* **30**: 1011-1017.

Li W, Zhou J, Lin Z, Hu Z (2007) Study on fermentation condition for production of huperzine A from endophytic fungus 2F09P03B of *Huperzia serrata*. *Chin Med Biotechnol* **2**:254–259.

Maria João Ramalho, Stephanie Andrade, Joana Angélica Loureiro, Maria do Carmo Pereira (2020) Nanotechnology to improve the Alzheimer's disease therapy with natural compounds. *Drug Delivery and Translational Research*, **10**: 380–402.

Olga Lidia Cruz-Miranda, Jorge Folch-Mallol, Fernando Martínez-Morales, Reinier Gesto-Borroto, María Luisa Villarreal & Alexandre Cardoso Taketa (2020) Identification of a Huperzine A-producing endophytic fungus from *Phlegmariurus taxifolius. Molecular Biology Reports* **47**: 489–495.

Orhan, I.E., Orhan, G., Gurkas, E. (2011) An overview on natural cholinesterase inhibitorsea multi-targeted drug classeand their mass production. *Mini. Rev. Med. Chem* **11**: 836-842.

Peng Y, Jiang L, Lee DY, Schachter SC, Ma Z, Lemere CA (2006) Effects of huperzine A on amyloid precursor protein processing and beta-amyloid generation in human embryonic kidney 293 APP Swedish mutant cells. *J Neurosci Res* **84**(4): 903–11.

Qian L, Ji R (1989) A total synthesis of (±)-huperzine A. *Tetrahedron Lett* **30**: 2089–2090.

Rafii MS, Walsh S, Little JT, Behan K, Reynolds B, Ward C, Jin S, Thomas R, Aisen PS (2011) A phase II trial of huperzine A in mild to moderate Alzheimer disease. *Neurology* **76**(16): 1389–94.

Ratia, M., Giménez-Llort, L., Camps, P., Muñoz-Torrero, D., Pérez, B., Clos, M.V., Badia, A. (2013) Huprine X and huperzine A improve cognition and regulate some neurochemical processes related with Alzheimer's disease in triple transgenic mice (3xTg-AD). *Neurodegener. Dis* **11**: 129-140.

Robert Perneczky (2018) Biomarkers for Preclinical Alzheimer's Disease. Humana Press, New York .

Shaohua Shu, Xinmei Zhao, Wenjuan Wang, Guowei Zhang, Andreea Cosoveanu, Youngjoon Ahn, Mo Wang (2014) Identification of a novel endophytic fungus from *Huperzia serrata* which produces huperzine A. *World J Microbiol Biotechnol* **30**: 3101–3109.

Shen P, Fan XR, Li GW (2000) The experiment of microbiology, 3rd version. Publishing House of High Education, China.

Shao H, Lv HF, Zhang L (2009) Research progress on original source plants of huperzine A. *J Shanghai Univ Tradit Chin Med* **23**: 83-86.

Stierle A, Strobel G, Stierle D (1993) Taxol and taxane production by T*axomyces andreanae*, an endophytic fungus of Pacific yew. *Science* **260**: 214-216.

Su JQ (2011) Alkaloid and Huperzine A Production from Endophytic Fungi isolated from *Huperziaceae*. M.A. dissertation. Fuzhou, Fujian Normal University, China (in Chinese).

Wang Y, Yan R-M, Zeng Q-G, Zhang Z-B, Wang D, Zhu D (2011) Producing huperzine A by an endophytic fungus from *Huperzia serrata*. *Mycosystema* **30**: 255–262.

Wei JC (1979) Fungal identification manual. Science Press, Beijing.

Wu X, Cai H, Pan L, Cui G, Qin F, Li Y, Cai Z (2019) Small Molecule Natural Products and Alzheimer's Disease. *Curr Top Med Chem* **19**(3):187-204.

Xiaoqiang Ma, David R. Gang (2008) In vitro production of huperzine A, a promising drug candidate for Alzheimer’s disease. *Phytochemistry* **69**: 2022-2028.

Xiao-Tian Huang, Zhong-Ming Qian, Xuan He, Qi Gong, Ka-Chun Wu, Li-Rong Jiang, Li-Na Lu, Zhou-jing Zhu, Hai-Yan Zhang, Wing-Ho Yung, Ya Ke (2014) Reducing iron in the brain: a novel pharmacologic mechanism of huperzine A in the treatment of Alzheimer's disease. *Neurobiology of Aging* **35**: 1045-1054.

Xia Y, Kozikowski AP (1989) A practical synthesis of the Chinese “nootropic'' agent huperzine A: a possible lead in the treatment of Alzheimer's disease. *J Am Chem Soc* **111**: 4116–4117.

Xu SS, Gao ZZ, Weng Z, Du ZM, Xu WA (1995) Efficacy of tablet huperzine-A on memory, cognition, and behavior in Alzheimer's disease. *Acta Pharmacologica Sinica* **16**(5): 391–395.

Ya Wang, Qing Gui Zeng, Zhi Bin Zhang, Ri Ming Yan, Ling Yun Wang, Du Zhu (2011) Isolation and characterization of endophytic huperzine A-producing fungi from Huperzia serrata. *J Ind Microbiol Biotechnol* **38**:1267–1278.

Ying Wang, Yanling Wei, Samuel Oguntayo, Bhupendra P. Doctor, Madhusoodana P. Nambiar(2013) A

combination of [+] and [-]Huperzine A improves protection against soman toxicity compared to [+]-Huperzine A in guinea pigs. *Chemico-Biological Interactions* **203**: 120-124.

Yuan Haidan, Ma Qianqian, Ye Li, Piao Guangchun (2016) The traditional medicine and modern medicine from natural products. Molecules 21(5) pii: E559. doi: 10.3390/molecules21050559.

Zelik P, Lukesova A, Voloshko LN (2009) Screening for acetylcholinesterase inhibitory activity in *cyanobacteria* of the genus Nostoc. *J Enzyme Inhib MedChem* **24**(2): 531-536.

Zhejian Wang, Zhao Ma, LiliWang, Chengchen Tang, Zhibi Hu, GuiXin Chou, Wankui Li (2015) Active anti-acetylcholinesterase component of secondary metabolites produced by the endophytic fungi of *Huperzia serrata*. *Electronic Journal of Biotechnology* **18**: 399-405.

Zhi Bin Zhang, Qing Gui Zeng, Ri Ming Yan, Ya Wang, Zheng Rong Zou, Du Zhu (2011) Endophytic fungus *Cladosporium cladosporioides* LF70 from *Huperzia serrata* produces Huperzine A. *World J Microbiol Biotechnol* **27**: 479–486.

Zhu D, Wang J, Zeng Q, Zhang Z, Yan R (2010) A novel endophytic huperzine A-producing fungus *Shiraia* sp. Slf14 isolated from *Huperzia serrata*. *J Appl Microbiol* **109**:1469–1478.

Figures

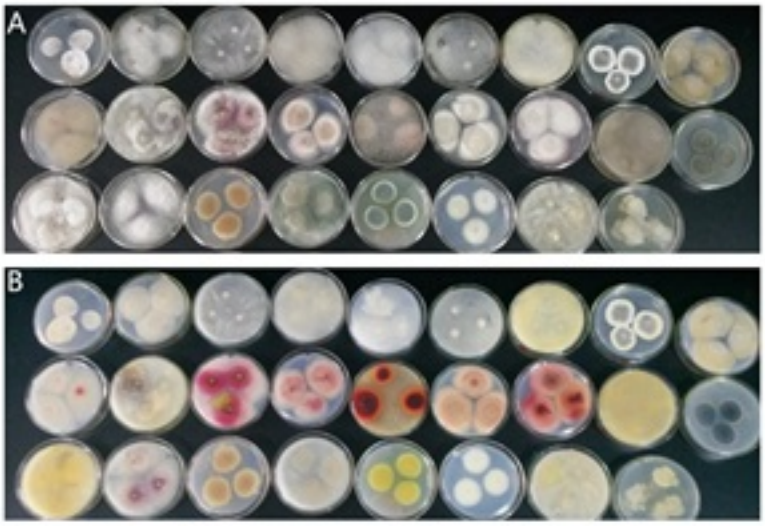

Figure 1

Endophytic fungi isolated from HS: the morphology of colony on the upside of PDA (A); the morphology of colony on the backside of PDA (B).

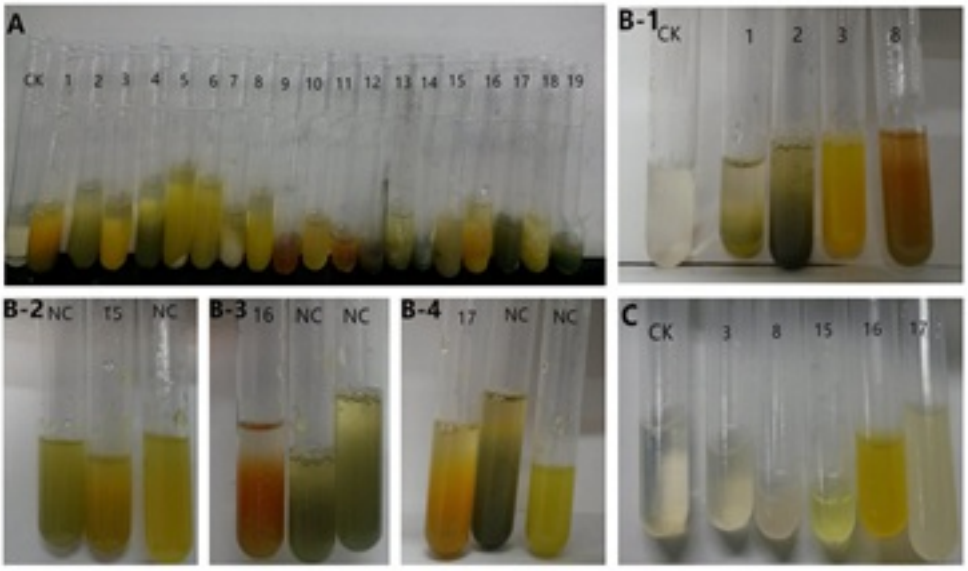

Figure 2

Results of the alkaloid precipitation tests. A: Detection of alkaloid by potassium mercuric iodide; B: Detection of alkaloid by bismuth potassium iodide; C: Detection of alkaloid by silicotungstic acid. CK: control check; NC: negative control. 1-19: the number of strain.

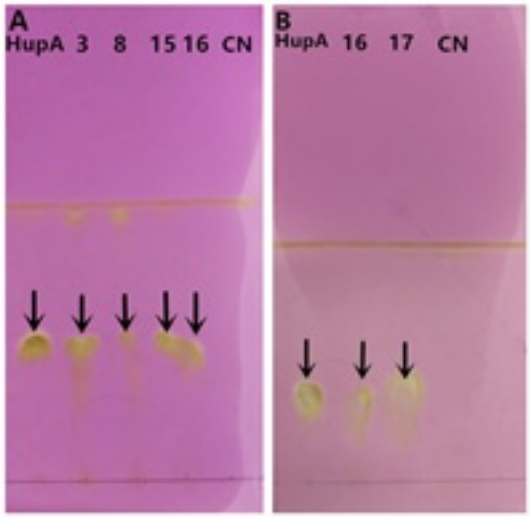

Figure 3

Results of the TLC tests. Strains of 3, 8, 15, 16 and 17: Detection of Huperzine A by TLC of endophytic fungi from HS; NC: Negative Control; HupA: TLC analysis of SHA; arrow indicates the presence of HupA.

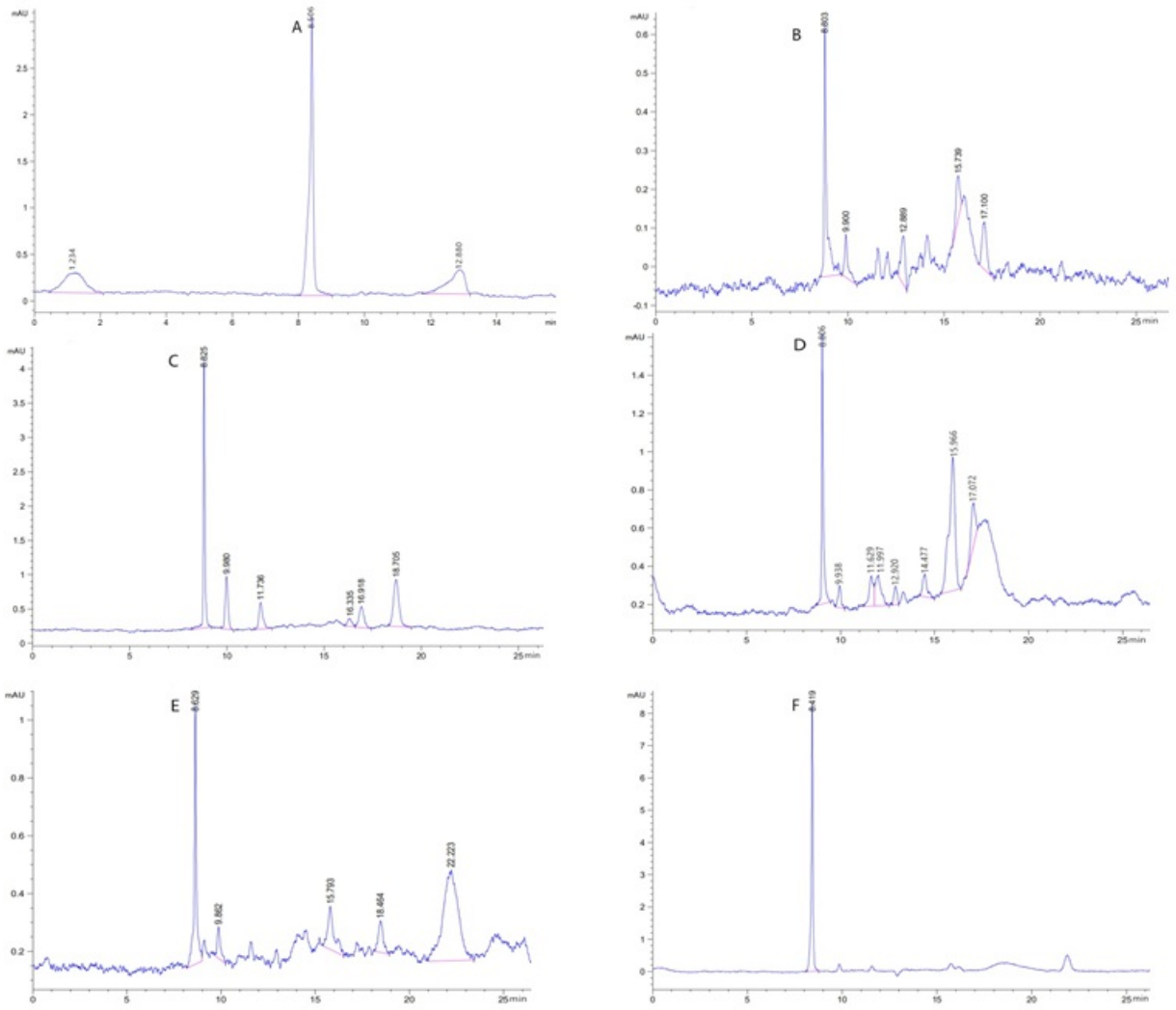

Figure 4

The registration of peak and retention time recorded by HPLC for the strains of 3 (B), 8 (C), 15(D), 16 (E) and 17(F). The SHA (A) as controls.

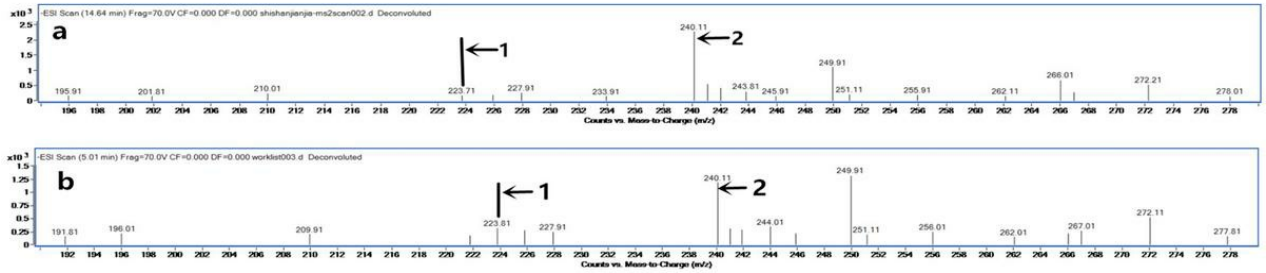

Figure 5

The chromatograms of LC-MS/MS for HupA. a: Standard huperzine A(SHA), arrow 1 indicates the molecularion of HupA at m/z 223.71 [M-NH2]-, arrow 2 indicates the molecularion of HupA at m/z 240.11 [M-H]-; b: HupA obtained from the fungus (FHA), arrow 1 indicates the molecularion of HupA at m/z223.81 [M-NH2]-, arrow 2 indicates the molecularion of HupA at m/z 240.11 [M-H]- .

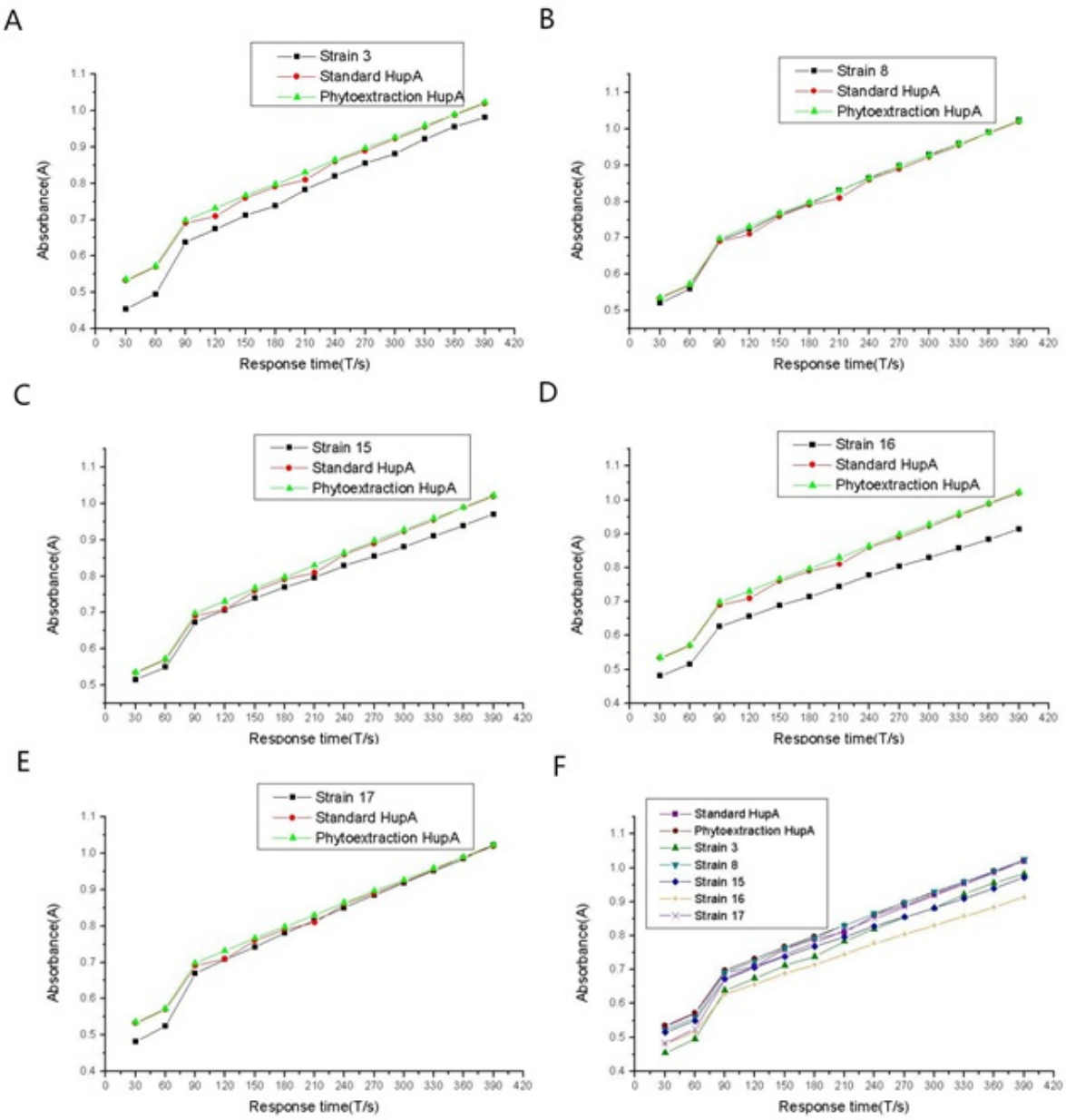

Figure 6

Inhibition activity of AChE of the biosynthetic HupA for the strains of 3 (A), 8 (B), 15(C), 16 (D), 17(E) and all (G). Each point represents the average of the three outcomes (n=3).

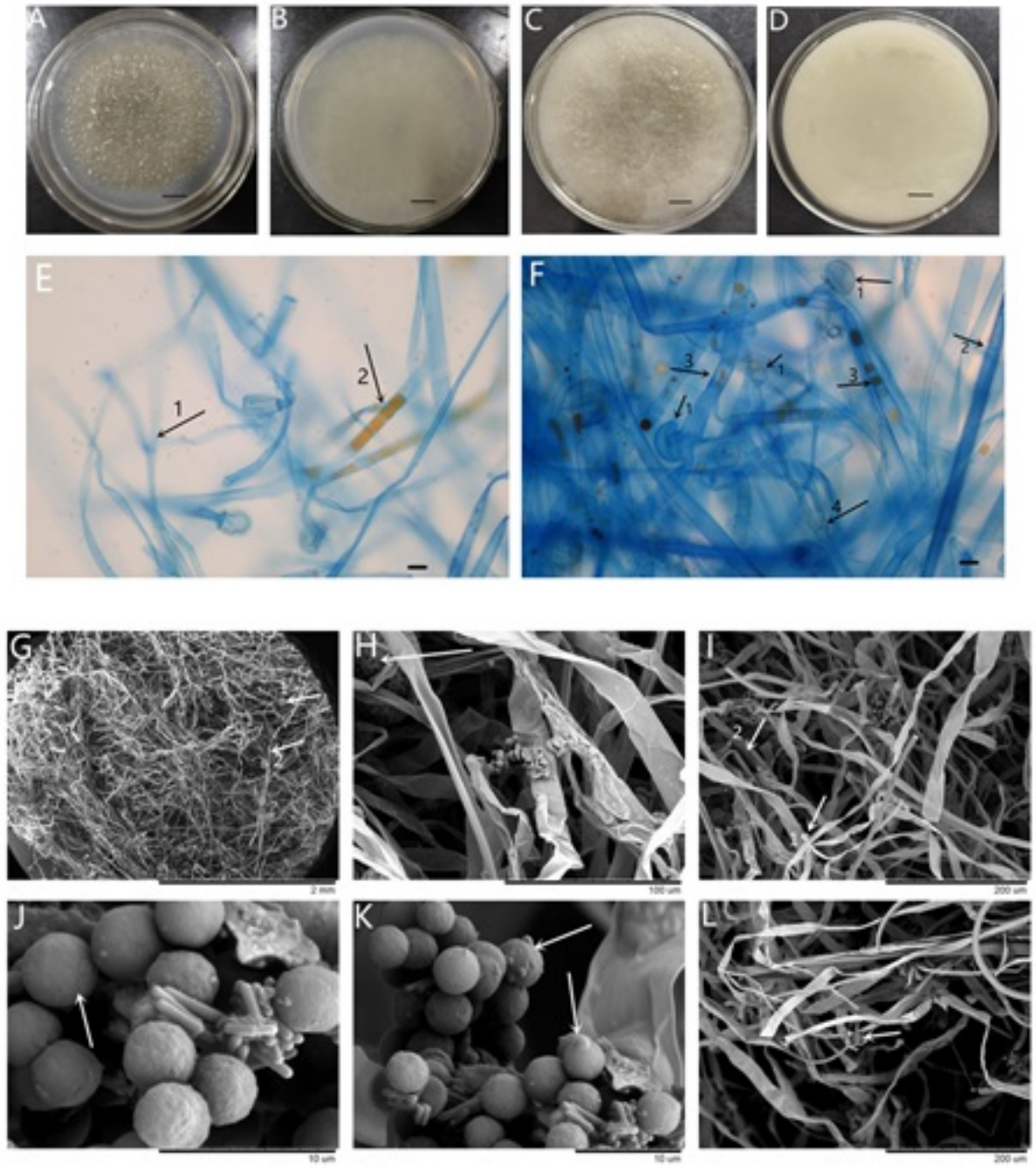

Figure 7

Morphological characteristics of NSH-D. A,B: colonial morphology of the upside and backside of PDA medium after 3 d; C,D: colonial morphology of the upside and backside of PDA medium after 5 d; E: sporangiophore with uniaxial branching and chlamydospore, 1: uniaxial branching sporangiophore, 2: chlamydospore; F: 1: spherical sporangium, 2: septahypha, 3: chlamydospore, 4: sporangiophore with uniaxial branching; G: 1: spherical sporangium, 2: septahypha; H: mature sporangium; I: 1: young sporangium, 2: chlamydospore in mycelium;

J: spore; K: spherical zygosperm with prominence; L: thallospore on the sporophore formed as short ova. E-F: screened by light microscope (40×10); G-L: screened by electron micrographs. A, B, C, D=100 mm; E, F=50 μm; J, K=10 μm; G=2 μm; H=100 μm; I, L=200 μm.

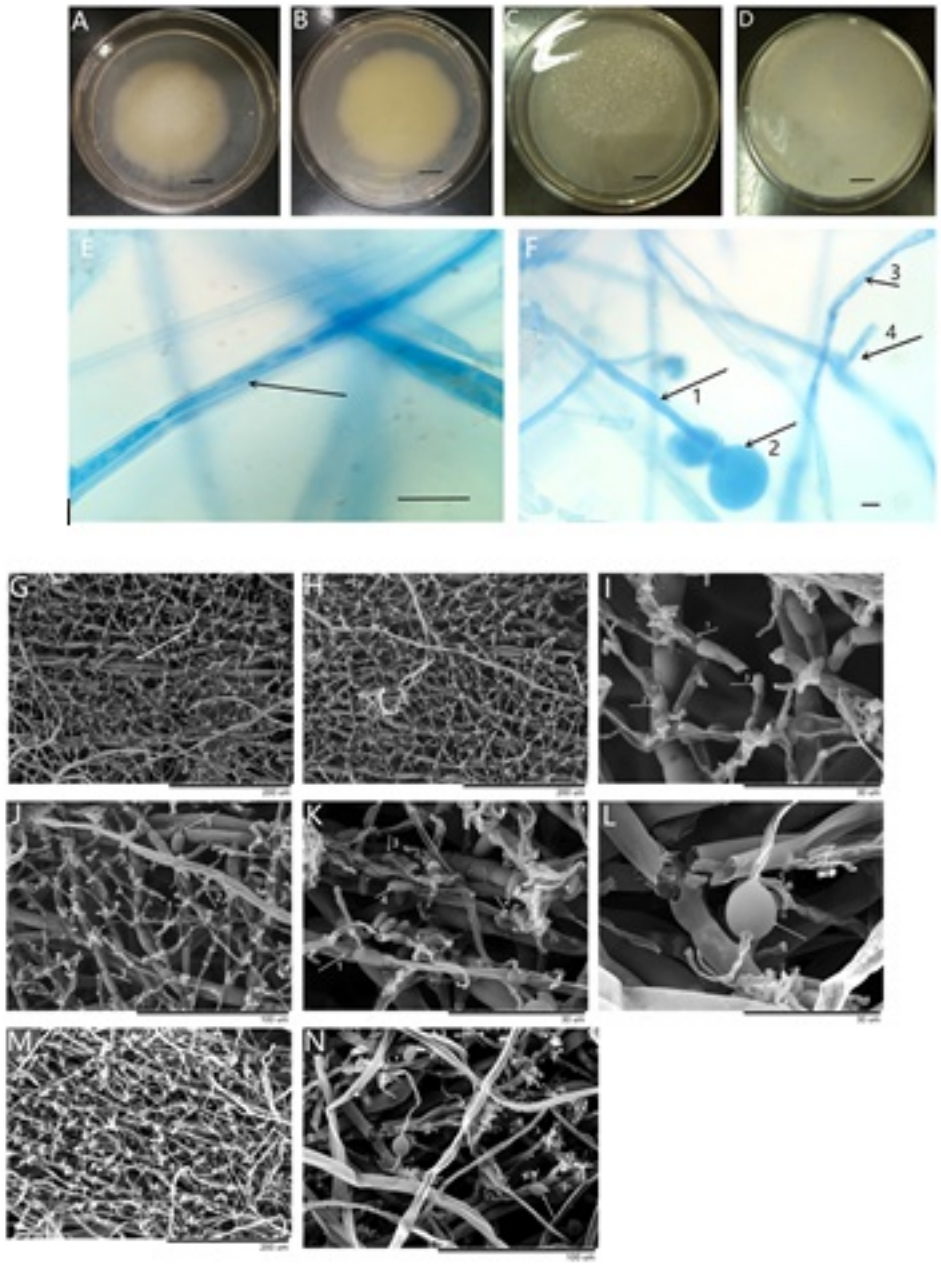

Figure 8

Morphological characteristics of NSY-1. A-D: forming white to brown colony on PDA at 28℃, A,B: the colony on the 3th day, C,D: the colony on the 4th day; E: aseptate hypha; F: single sporophore standing upright look like long cylinders diameter of 1-2 cm×30-50 μm,

acrogenous sporangium, with no sterigmata branch, 1: sporophore, 2: acrogenous sporangium, 3: aseptate hypha, 4: short branch of sporangiole appear occasionally from the stem base of sporophore; G: sporophore; H: short branch of sporangiole appear occasionally from the stem base of sporophore; I: thin-wall sporangium and variegated sporangiospor, 1: thin-wall sporangium, 2: spherical spores, 3: oval spores; J: sporangiospore, 1,3: thin-wall sporangium containing cylindrical conidium, 2: conidium appeared to be string; K: conidium, 1: conidium was released after the thin-wall sporangium fracture, 2: spherical conidium (diameter 1-1.5 μm), 3: oval conidiun (aspect ratio of 2:1, size is 6×3 μm), 4: oval conidium (aspect ratio of 2:1, size is 9×3 μm); L: zygosperm came from hypha, arrow behalf of zygamgium had been completed the process of zygo; M: zygosperm came from hypha, arrow behalf of zygamgium was going to zygo; N: chlamydospore, smooth and colorless, usually acrogenous. E-F: screened by light microscope (100×10); G-N: screened by electron micrographs. A, B, C, D=100 mm; E, F=50 μm; G, H, M=200 μm; I, K, L=30 μm; J, N=100 μm.

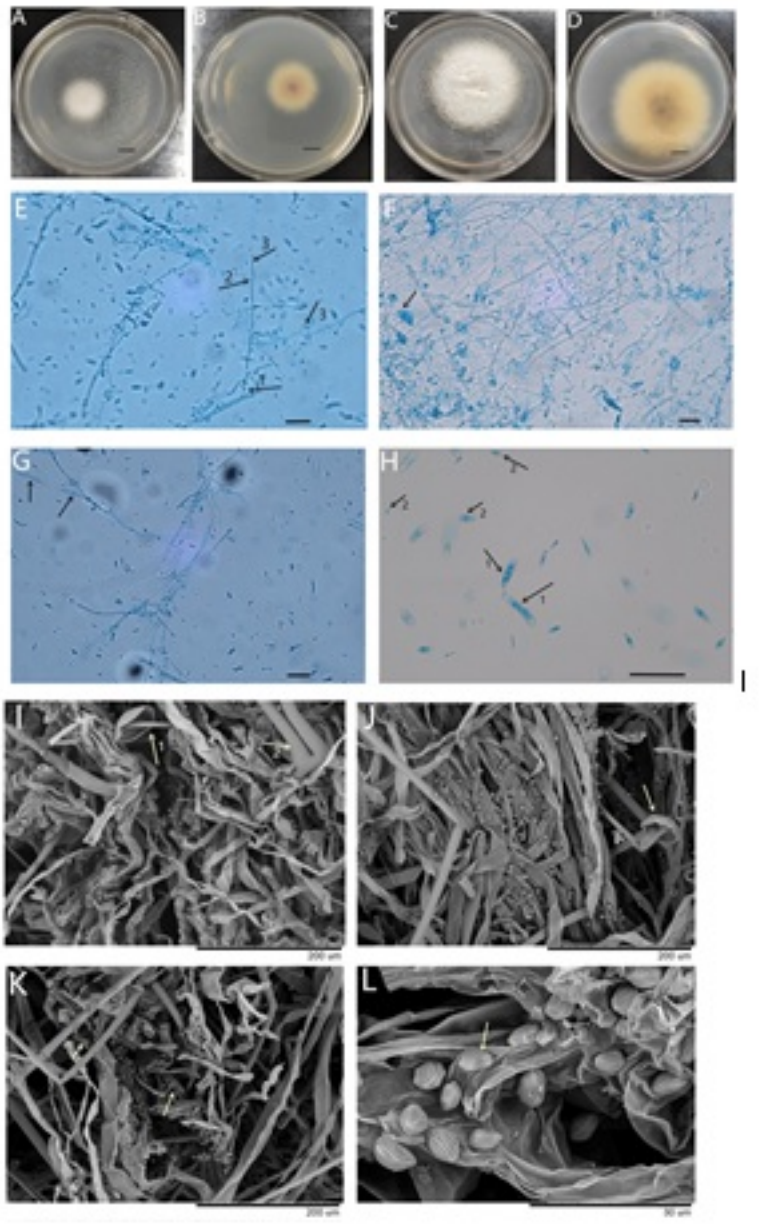

Figure 9

Morphological characteristics of NSH-5. A-D: forming dense, developed and cotton-like colony on PDA at 28℃, A,B: the colony on the 3th day, C,D: the colony on the 5th day; E: conidiophore, 1: born from the aerial mycelium, 2: rotate-branched conidiophore, 3: apical conidia arranged in chains; F: conidia arranged in chains; G: septate hypha; H: different size of conidia, 1: the few great conidia, 2: numerous microconidia; I: false heads and conidiophore, 1: false heads, 2: conidiophore born from aerial mycelium; J: false heads; K,L: microconidium. E-G: screened by light microscope (40×10), H: screened by light microscope (100×10); I-L: screened by electron micrographs. A, B, C, D=100 mm; E, F, G, H=50 μm; I, J,

K=200 μm; L=30 μm.

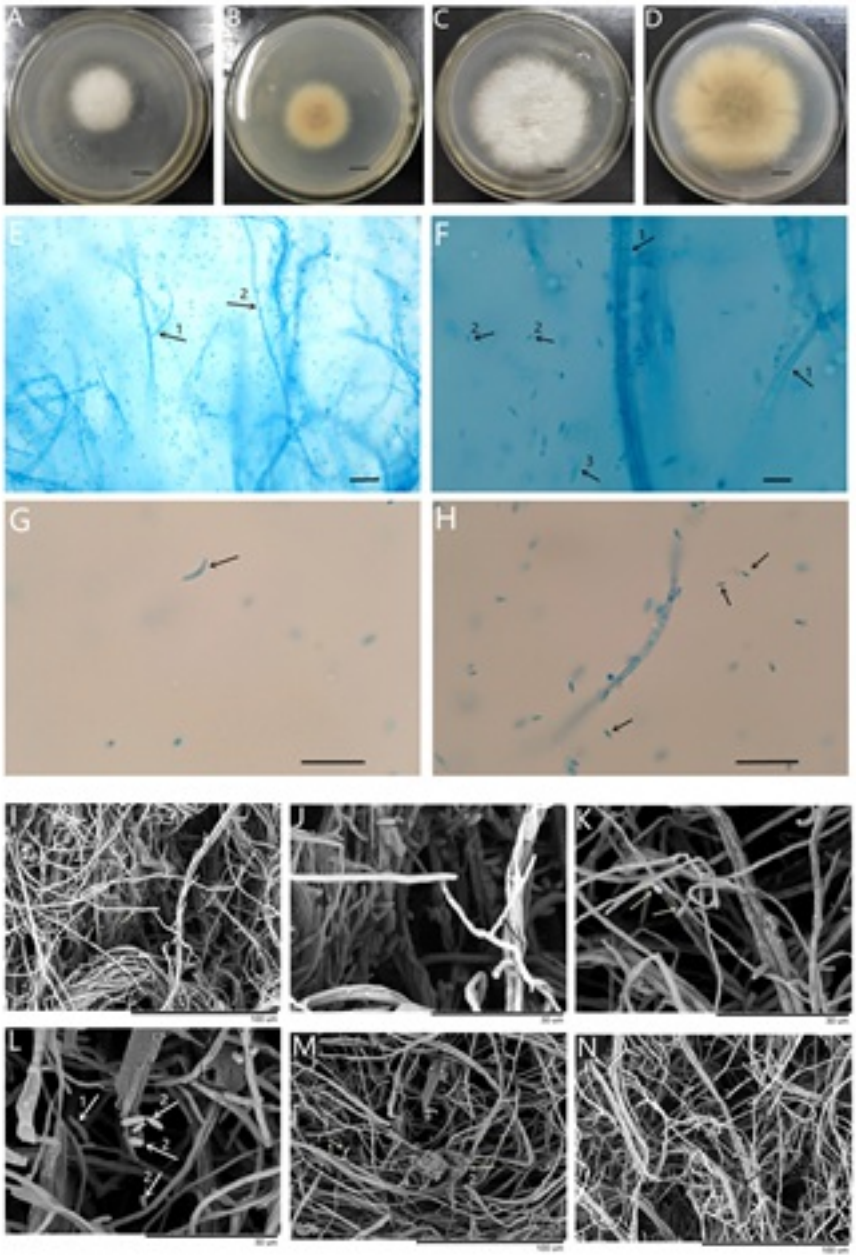

Figure 10

Morphological characteristics of NSG-1. A-D: forming dense, developed and cotton-like colony on PDA at 28℃, A,B: colonial morphology of the upside and backside of PDA medium after 3d; C,D: colonial morphology of the upside and backside of PDA medium after 5d; E: conidiophore, 1: rotate-branched conidiophore, 2: unbranched conidiophore; F: septate hypha and conidia , 1: Septate hypha, 2: microconidia, 3: scattered great conidia; G: scattered great conidia; H: microconidia; I: unbranched conidiophore; J: conidiophore born

from aerial mycelium; K: microconidia inserted on the apex of a single conidiophore; L: different size of conidia, 1: the few great conidia, 2: numerous microconidia; M,N: apical chlamydospore. E□screened by light microscope (40×10), F-H: screened by light microscope (100×10); I-N: screened by electron micrographs. A, B, C, D=100 mm; E, F, G, H=50 µm; I, M, N=100 µm; K, J, L=30 µm.

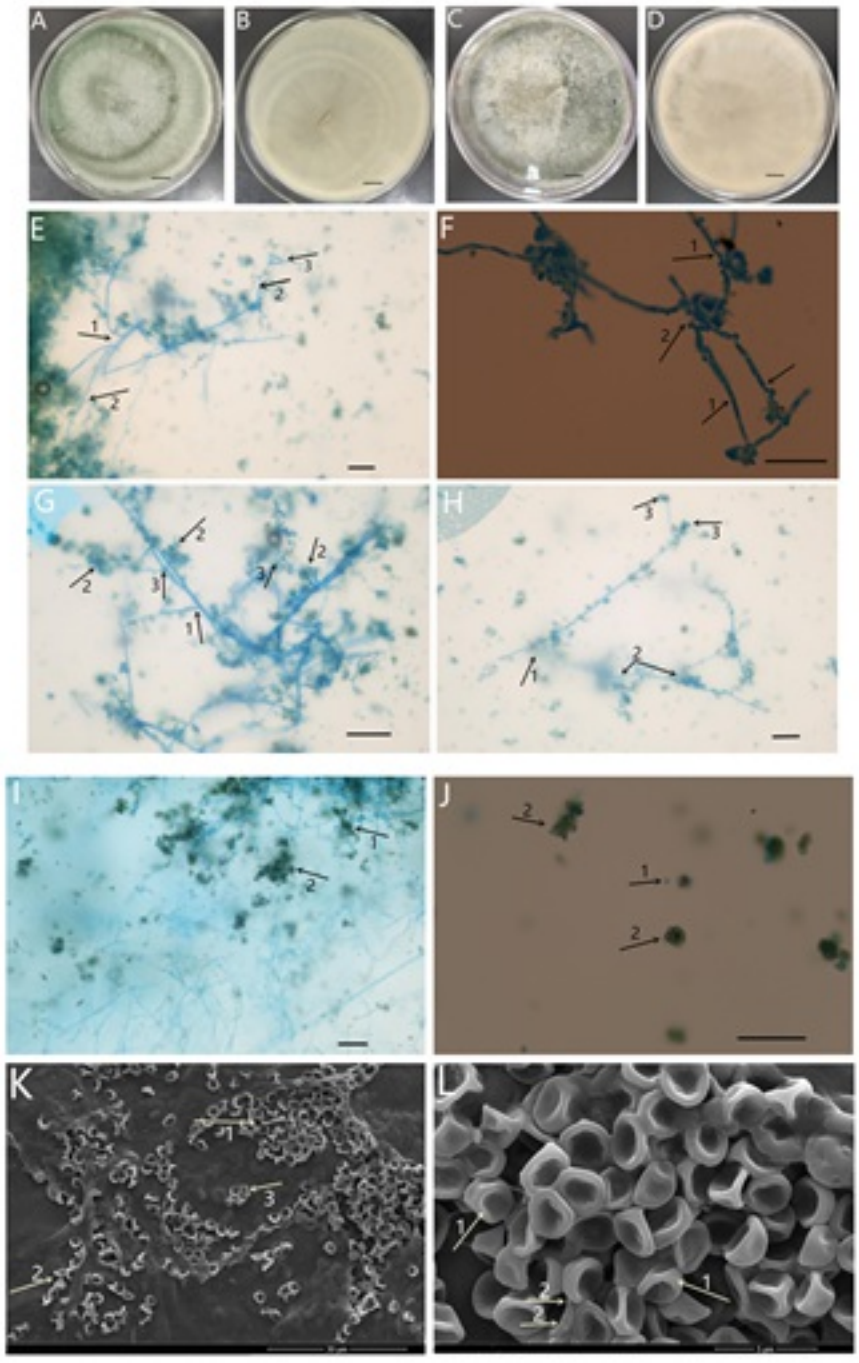

Figure 11

Morphological characteristics of NSW-V. A-D: forming intensive and felt-like colony on PDA at 28℃, A,B: colonial morphology of the upside and backside of PDA medium after 4 d; C,D: colonial morphology of the upside and backside of PDA medium after 7 d; E: conidiophore, 1: born from the lateral branches of aerial hyphae, 2: alternate conidiophore, 3: opposite conidiophore; F: hypha, 1: septate hypha, 2: hypha with many branches; G: conidiophore, 1: alternate conidiophore, 2: the upper conidia head, 3: opposite conidiophore; H: conidiophore, 1: bifurcate conidiophore, 2: alternate conidiophore, 3: the upper conidia head; I: minor conidiophore, 1: bottle-shaped, 2: cone-shaped; J: conidium, 1: scattered conidia, 2: aggregated conidia; K: minor conidiophore and conidium, 1: minor conidiophore shaped as cone containing many condia 2: minor conidiophore shaped as bottle containing many condia, 3: scattered conidia; L: conidium, 1: spherical conidium, 2: conidium with small warts on the spore walls. E-I: screened by light microscope (40×10), J: screened by light microscope (100×10); K-L: screened by electron micrographs. A, B, C, D=100 mm; E, F, G, H, I, J=50 μm; K=30 μm; L=5 μm.

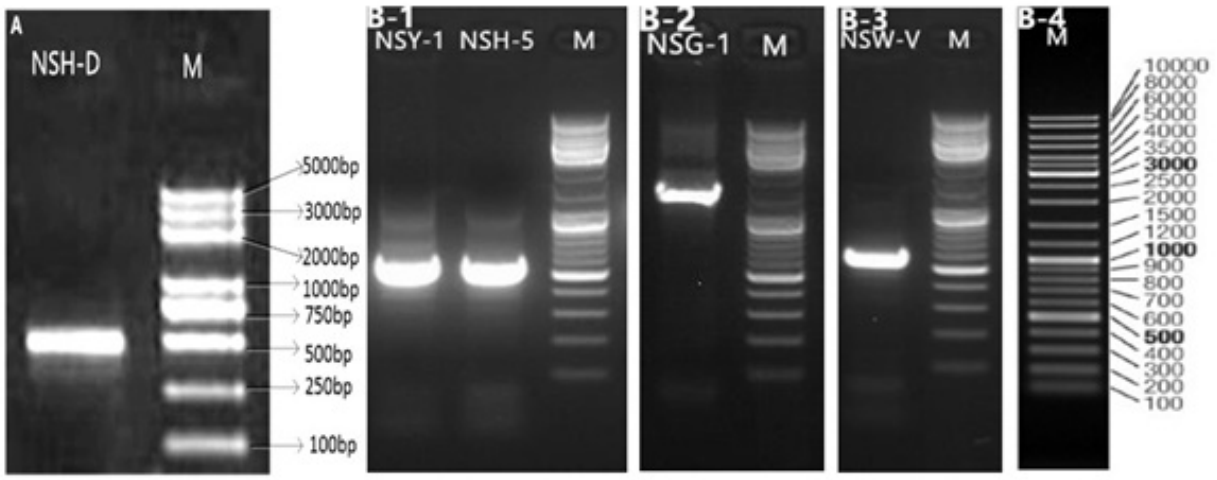

Figure 12

PCR amplification and agarose gel electrophoresis. A: lane 1: strain NSH-D, lane 2: marker1 (100-5000 bp); B-1: lane 1: strain NSY-1 and NSH-5, lane 2: marker2 (100-10000 bp); B-2: lane 1: strain NSG-1, lane 2: marker2 (100-10000 bp); B-3: lane 1: strain NSW-V, lane 2: marker2 (100-10000 bp); B-4: marker2 (100-10000 bp).

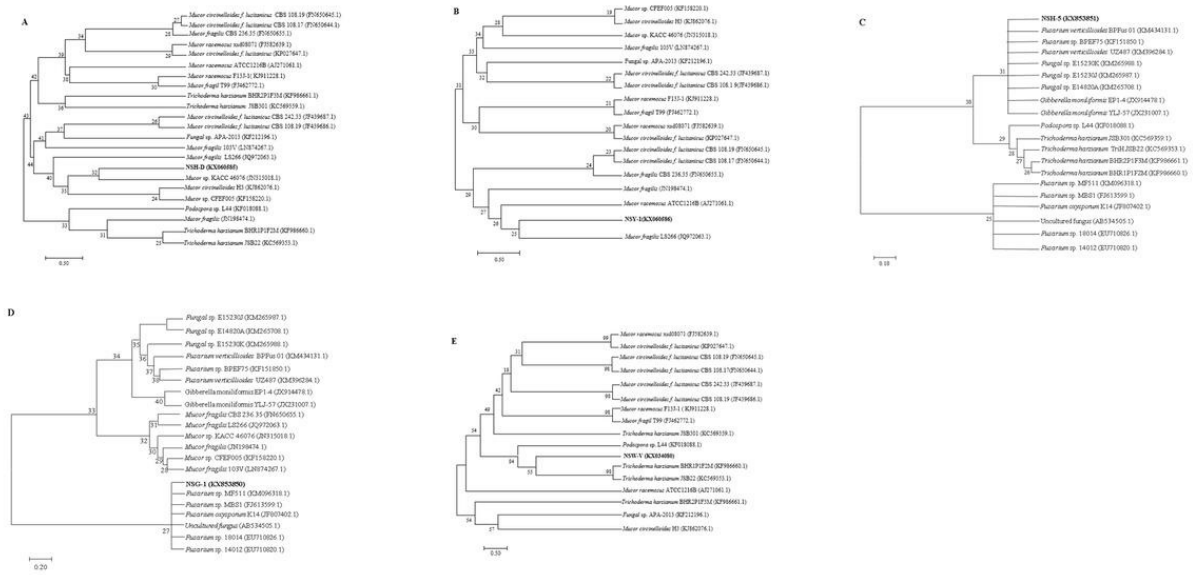

Figure 13

The phylogenetic trees constructed from ITS DNA for strains of NSH-D, NSY-1, NSH-5, NSG-1, NSW-V and collected from GenBank. The evolutionary history was inferred using the Neighbor-Joining method. The bootstrap consensus tree inferred from 1 000 replicates was taken to represent the evolutionary history of the taxa analyzed. Branches corresponding to partitions reproduced in less than 50% bootstrap replicates were collapsed. The percentage of replicate trees in which the associated taxa clustered together in the bootstrap test (1 000 replicates) was shown next to the branches. Evolutionary analyses were conducted in MEGA7.